

---

# Decision Trees with Dynamic Graph Features

---

**Maya Bechler-Speicher**  
Blavatnik School of Computer Science  
Tel-Aviv University  
Tel-Aviv, Israel

**Amir Globerson**  
Blavatnik School of Computer Science  
Sagol School of Neuroscience  
Tel-Aviv University  
Tel-Aviv, Israel

**Ran Gilad-Bachrach**  
Department of BioMedical Engineering  
Edmond J. Safra Center for Bioinformatics  
Tel-Aviv University  
Tel-Aviv, Israel

## Abstract

When dealing with tabular data, models based on decision trees are a popular choice due to their high accuracy on these data types, their ease of application, and explainability properties. However, when it comes to graph-structured data, it is not clear how to apply them effectively, in a way that incorporates the topological information with the tabular data available on the vertices of the graph. To address this challenge, we introduce Decision Trees with Dynamic Graph Features (TREE-G). Rather than only using the pre-defined given features in the data, TREE-G acts on *dynamic features*, which are computed as the graph traverses the tree. These dynamic features combine the vertex features with the topological information, as well as the cumulative information learned by the tree. Therefore, the features adapt to the predictive task and the graph in hand. We analyze the theoretical properties of TREE-G and demonstrate its benefits empirically on multiple graph and node prediction benchmarks. In these experiments, TREE-G consistently outperformed other tree-based models and often outperformed other graph-learning algorithms such as Graph Neural Networks (GNNs) and Graph Kernels, sometimes by large margins. Finally, we also provide an explainability mechanism for TREE-G, and demonstrate that it can provide informative and intuitive explanations.

## 1 Introduction

Decision Trees (DTs) are one of the cornerstones of modern data science and are a leading alternative to neural networks, especially in tabular data settings, where DTs often outperform deep learning models [1–4]. DTs are popular with practitioners due to their ease of use, out-of-the-box high performance, and explainability properties. In a large survey conducted by Kaggle<sup>1</sup> in 2022 with 23,997 data scientists worldwide, 63% of the participants reported using decision trees, Random Forests (RF) or Gradient Boosted Trees (GBT) on a regular basis [5–7].

Graph structured data are found in diverse domains including social studies, molecular biology, drug discovery, and communication [8, 9]. The ability to perform regression and classification on graphs is important in these domains and others, which explains the ongoing efforts to develop machine learning algorithms for graphs [10–21].

---

<sup>1</sup><https://www.kaggle.com/competitions/kaggle-survey-2022/data>

In many cases, features of the graph data are provided in tabular form. For example, the vertices of a social network are people with associated features such as age, place of residence, education, etc. Given the popularity and advantages of DTs in other machine learning tasks, it makes sense that they would be popular for graph-related tasks as well, especially when the graphs are based on tabular data. Unfortunately, it turns out that applying DTs to graphs effectively is challenging. To respond to this need, we propose a novel, effective approach for applying DTs on graphs.

DTs split the input space by asking questions about the values of features. When operating on graphs, these questions must incorporate the features on the vertices<sup>2</sup> of the graph as well as its topological structure. Moreover, these questions should be invariant to the varying sizes of different graphs and the way in which the graph is represented (permutation invariance and equivariance). To apply decision trees to graph data, current methods extract pre-defined features based on the graph information and add them to the 'raw features' (a process sometimes called 'feature engineering'). These features, which are computed in advance, are usually based on prior knowledge, or inspired by graph theory [22, 23]. However, these approaches are labor intensive, require domain knowledge, and may fail to capture interactions between vertex features and graph structure, as we prove below.<sup>3</sup>

The success of DTs on tabular data suggests that they can potentially perform well on graph data, given appropriate design modifications to capture the graph structure. Towards this end, we introduce Decision Trees with Dynamic Graph Features (TREE-G), a novel method for applying DTs on graph data. TREE-G can be applied to directed and undirected graphs of arbitrary sizes and perform classification, regression, and other prediction tasks on entire graphs or on the vertices and edges of these graphs. In an extensive empirical evaluation, we demonstrate the superiority of TREE-G over existing tree-based methods. We show that TREE-G often outperforms Graph Neural Networks, the leading deep-learning method for learning over graphs. This is achieved by simple decision trees without the sophistication of deep learning. In some cases, the difference in performance between TREE-G and the other methods examined reaches  $\sim 6.4$  percentage points.

The key idea in TREE-G is to allow the tree to explore substructures of the graph, in a dynamic manner. This is motivated by the fact that even when predicting the properties of entire graphs, it is sometimes important to focus on substructures of these graphs. For example, the tendency of a molecule to change genetic material and increase mutation frequency is known to be related to the presence of certain substructures in the molecule such as ring (cycle) groups [24]. When these task-related substructures are known in advance, it is possible to compute task-specific features based on these sub-structures. However, when the sub-structures are not known in advance it is not clear how to compute features based on, say, sub-graphs, in a way that is both computationally efficient and consistent across different graphs. To address this problem, TREE-G uses a novel concept dubbed *dynamic features*, which are generated as the graph traverses the decision tree. These dynamic features combine the vertex features, the topology of the graph, and information from previous splits. TREE-G have the nontrivial ability to focus on substructures in the graph in an efficient manner. Ablation studies we performed confirmed that this ability is a key ingredient of the empirical superiority of TREE-G over other models. As we prove later, TREE-G is more expressive than standard decision trees that only act on the input features, even if some topological features which are computed in advance are added as input features.

**The main contributions** of this work are: (1) We present TREE-G, a new type of decision tree model specialized for graph data, that uses a novel concept of dynamic features. (2) We empirically show that TREE-G based ensembles outperform existing tree-based methods and graph kernels. Further, TREE-G is very competitive with GNNs and often outperforms them. (3) We provide theoretical results that highlight the properties and expressive power of TREE-G. (4) We introduce an explainability mechanism, which highlights the vertices and edges in the graph that contribute to the prediction.

## 2 Related Work

**Machine Learning on graphs** Many methods for learning on graphs have been proposed. One important line of works are Graph Kernel methods which measure the similarity between two graphs

<sup>2</sup>For the sake of clarity, we ignore edge-features in this work.

<sup>3</sup>This problem is demonstrated in Lemma 4.3 where a pair of non-isomorphic graphs over 4 vertices and 2 features are shown to be inseparable by standard tree methods.

by creating vector representations of graphs and computing their cosine similarities [18, 19, 25]. A more recent line of work utilizes deep-learning approaches: Graph Neural Networks (GNNs) learn a representation vector for the vertices of a given graph using an iterative neighborhood aggregation process. These representations are used in downstream tasks [9, 16, 17, 26–31]. See Wu et al. [32], Zhou et al. [33], and Nikolentzos et al. [34] for recent surveys.

**DTs for graph learning** Several approaches have been introduced to allow DTs to operate on graphs [22, 23, 35–39]. These approaches combine domain-specific feature engineering with graph-theoretic features. Other approaches combine GNNs with DTs in various ways and have mostly been designed for specific problems [40]. For example, XGraphBoost was used for a drug discovery task [41, 42]. It uses GNNs to embed the graph into a vector and applies GBT [6, 7] to make predictions using this vector representation. A similar method has been used for link prediction between human phenotypes and genes [43]. The recently proposed BGNN model predicts vertex attributes by alternating between training GBT and GNNs [44]. Thus, existing solutions either combine deep-learning components, or focus on specific domains that require domain expertise.

TREE-G, which is presented in the following section, attempts to provide a “pure” DT solution specialized for graph-based tasks that does not require domain knowledge or the use of deep-learning procedures, while being competitive with these methods.

In Set-Trees [45] DTs were extended to operate on data that had a set structure by introducing an attention mechanism. Sets can be viewed as graphs with no edges. Thus, Set-Trees are used as the inspiration for the current work. However, note that since Set-Trees are designed to work on sets, they do not provide any way to integrate the topological structure of graphs or the diverse types of tasks that graph data gives rise to such as graph prediction, vertex prediction, or link prediction.

### 3 Dynamic Graph Features

In this section we introduce TREE-G, a method for learning decision trees on graph data.

#### 3.1 Preliminaries

A graph  $G$  is defined by a set of vertices  $V$  of size  $n$  and an adjacency matrix  $A$  of size  $n \times n$  that can be symmetric or a-symmetric. In our notation, the entry  $A_{ij}$  indicates an edge from vertex  $j$  to vertex  $i$ , and vertex  $j$  is a neighbor of vertex  $i$  if  $A_{ij} = 1$ . We assume that each vertex is associated with a vector of  $l$  real-valued features, and denote the stacked matrix of feature vectors over all the vertices by  $X$ . We denote the  $k$ ’th column of this matrix by  $\mathbf{f}_k$ ; i.e., entry  $i$  in  $\mathbf{f}_k$  holds the value of the  $k$ ’th feature of vertex  $i$ . The  $i$ ’th entry of a vector  $\mathbf{x}$  is denoted by  $x_i$  or  $(\mathbf{x})_i$ . To indicate multiple entries, we similarly use a subscript with the set of entries; e.g.  $(\mathbf{x})_{\{1,2\}}$ . Recall that  $(A^d)_{ij}$  is the number of walks of length  $d$  between vertex  $j$  to vertex  $i$ . We focus on two tasks: *graph labeling* and *vertex labeling* (each includes both classification and regression). In the former, the goal is to assign a label to the entire graph while in the latter, the goal is to assign a label to individual vertices.<sup>4</sup> In vertex labeling tasks TREE-G receives a graph and one of its vertices and predicts the label of the vertex whereas in graph labeling tasks TREE-G receives a graph and predicts the label of the entire graph. Since there are different types of graph tasks TREE-G has different flavors. Trees are graphs as well. Hence to avoid confusion we refer to the decision tree nodes as *root*, *node*, *split-node*, *leaf*, and to the graph vertices as *vertex*, *vertices*.

#### 3.2 Dynamic Graphs Features

In standard decision trees, the goal is to classify an input  $\mathbf{x}$  based on its features  $x_1, \dots, x_l$ . Given  $\mathbf{x}$ , the tree is traversed by asking at each split-node whether  $x_k > \theta$  for some feature index  $k$  and a threshold  $\theta$ . When a leaf is reached, the value stored in it is reported. In TREE-G, instead of querying the value of a feature, the algorithm queries the value of a *dynamic feature*, which combines the vertex-features, the adjacency matrix of the graph, and a subset of the vertices determined by previous splits in the tree. Therefore, the selected feature at each split-node will depend on a subset of the graph. To achieve this, in TREE-G each split-node also partitions the vertices of the graph into two

<sup>4</sup>Tasks that require predicting properties of edges, can be represented as vertex labeling tasks using a line graph as we describe in the appendix.

subsets. Then, each split-node can use a subset that was created in one of its ancestors in the tree. Technically, while in standard decision trees the feature is only parameterized by its index  $k$ , the dynamic features used in TREE-G are parameterized by 5 parameters  $k, d, u, r$  and  $\rho$ , as explained in Section 3.2.1. Therefore, the question at a given split-node in the tree takes the form  $\phi_{k,d,u,\rho,r} > \theta$ , where  $\phi_{k,d,u,\rho,r}$  is the function that computes the dynamic-feature. The parameters  $u$  and  $\rho$  uniquely define a subset of vertices, and together with the parameter  $r$ , they allow the question asked in the split-node to focus on a subset of the graph instead of the whole graph. The parameters  $k, d$  specify how the input vertex features are combined with the graph. For the sake of clarity, we first focus on vertex labeling, and explain graph labeling in Subsection 3.5.

### 3.2.1 TREE-G for vertex labeling

In vertex labeling, each example is a vertex in the graph. The question asked at a split-node in TREE-G is based on a feature  $k$  propagated through walks of length  $d$ , over parts of the graph. For example, for some vertex example in a graph, the question may be: is the sum of the  $k^{\text{th}}$  feature over my neighbors greater than  $\theta$ ? We begin by explaining how this is calculated for the whole graph. To efficiently propagate features over walks in the graph, we use the function  $A^d \mathbf{f}_k$ . Therefore, the parameters  $d$  and  $k$  are used to propagate the  $k^{\text{th}}$  feature through walks of length  $d$  in the graph. For example, the  $i^{\text{th}}$  entry in  $A^1 \mathbf{f}_k$  is the sum of the values of the  $k^{\text{th}}$  feature over the neighbors of the  $i^{\text{th}}$  vertex. If  $d = 0$ , then  $A^0 \mathbf{f}_k = \mathbf{f}_k$ ; namely, the graph structure is ignored. If  $\mathbf{f}_0$  is the constant feature 1, then  $(A^d \mathbf{f}_0)_i$  is the number of walks of length  $d$  that end in vertex  $i$ .<sup>5</sup>

Next we describe how we limit the walks solely to a subset of the vertices. Given a subset of vertices  $S$ , we would like to adapt the values of  $A^d \mathbf{f}_k$  to focus on this subset. This implies that the calculated value of the dynamic feature is based on a substructure in the graph, rather than the whole graph. There are many ways in which we can restrict walks based on  $S$ . Below we present methods that are natural and computationally effective.<sup>6</sup>

1. **Source Walks:** Only consider walks starting in the vertices in  $S$ .
2. **Cycle Walks:** Only consider walks starting and ending in the same vertex in  $S$ .

These restrictions, can be implemented simply by zeroing out parts of the walks matrix  $A^d$ , before propagating the feature values  $\mathbf{f}_k$ . For source walks, zero out the  $j^{\text{th}}$  column in  $A^d$  for each vertex  $j \notin S$ . For cycle walks, zero out all  $A^d$  except for the  $j^{\text{th}}$  value on the main diagonal, for each vertex  $j \in S$ .

The key challenge is to design a policy to select the set  $S$ . Clearly, we cannot add  $S$  as a feature that the DT enumerates over, since there are exponentially many and their definition would not generalize across different graphs. Our main insight is that the set  $S$  cannot be determined before the graph  $G$  on which to operate is provided. Therefore, we propose to generate  $S$  dynamically based on previous split-nodes in the tree. In TREE-G, each split-node not only splits the data, but also uses its selected parameters to generate two subsets of the vertices. We denote the two generated subsets at a split-node  $v$  to be  $S_{v,+}$  and  $S_{v,-}$ , and will later explain how they are generated in Section 3.3. Next, we present the expression for the split function  $\phi$ , assuming that subsets have been generated for all its ancestors in the tree.

Every split-node in the tree uses one of the subsets generated by its ancestors in the tree, as follows. Formally, every split-node has parameters  $u, \rho$  that specify how to obtain its subset  $S_{u,\rho}$ . The parameter  $u$  is a pointer indicating which ancestor to take the generated subset from, and  $\rho \in \{+, -\}$  indicates if the chosen subset is  $S_{u,+}$  or  $S_{u,-}$ . Given a graph, values for  $u$  and  $\rho$  uniquely well-define a subset of its vertices  $S_{u,\rho}$ . We always allow each split-node to focus on the whole graph by selecting  $V$  itself as the subset. Therefore if the value of the pointer  $u$  is the split-node itself, the used subset is  $V$ , regardless of the value of  $\rho$ . Since the root node has no ancestors, the root node always points to itself and therefore uses all the vertices as a subset. For ease of notation, we limit  $A^d$  to the set  $S_{u,\rho}$  using a mask matrix that corresponds to one of the two options described above (i.e., source or cycle walks), and denote it by  $M_r(S_{u,\rho})$ ,  $r \in \{1, 2\}$ . The parameter  $r$  indicates the type of walk restrictions,

<sup>5</sup>In directed graphs it may be useful to consider negative  $d$  values to consider walks in the opposite direction.

<sup>6</sup>Specifically, the option we consider reduces the number of matrix powers that need to be calculated. See more in the Appendix.

where  $r = 1$  indicates source walks and  $r = 2$  indicates cycle walks. We apply  $M_r(S_{u,\rho})$  to  $A^d$  using an element-wise multiplication denoted by  $\circ$ .

Thus, given a vertex  $i$ , the adjacency matrix  $A$  of its graph, and the stacked feature vectors of the graph's vertices  $X$ , TREE-G computes a dynamic feature defined as follows:

$$\phi_{k,d,u,\rho,r}(A, X, i) = \left( \left( A^d \circ M_r(S_{u,\rho}) \right) \mathbf{f}_k \right)_i \quad (1)$$

Finally, the split criterion at a split-node will be given by the binary function:

$$\phi_{k,d,u,\rho,r}(A, X, i) > \theta \quad (2)$$

### 3.3 Subsets Generation

As mentioned above, each split-node  $v$  generates two subsets of the vertices  $S_{v,+}$  and  $S_{v,-}$ , which can be used by its descendant split-nodes in the tree. We now describe how these subsets are dynamically computed during the expansion of the tree. The split criterion in a split-node  $v$  uses some chosen parameters  $k, d, u, \rho$  and  $r$ , and a threshold  $\theta$ . In particular, it uses some selected subset of vertices  $S_{u,\rho}$ , where  $u$  is a pointer to an ancestor of  $v$  in the tree. Then, the generated subset  $S_{v,+}$  is simply the vertices among  $S_{u,\rho}$  that satisfy the criterion in Eq. 2 with the selected parameters and threshold. Similarly, the generated subset  $S_{v,-}$  is the vertices among  $S_{u,\rho}$  that did not satisfy the criterion. Formally, a split-node  $v$  generates two subsets, by partitioning its selected subset  $S_{u,\rho}$  into two new subsets:

$$S_{v,+} = \{j | \phi(A, X, j) > \theta, j \in S_{u,\rho}\}$$

and

$$S_{v,-} = \{j | \phi(A, X, j) \leq \theta, j \in S_{u,\rho}\}$$

We dropped the parameterization of  $\phi$  for brevity. In particular, it holds that  $S_{v,+} \cap S_{v,-} = \emptyset$  and  $S_{v,+} \cup S_{v,-} = S_{u,\rho}$ . The rationale is that vertices in  $S_{v,+}$  contribute towards satisfying the condition  $\phi > \theta$  whereas vertices in  $S_{v,-}$  do not.

Figure 1 demonstrates how subsets are generated while the graph traverses the tree. To the right of each split-node, are the subsets considered in that split-node, where the selected subset is marked with a rectangle. To the left of each split-node, are the two generated subsets, which are a partition of the selected subset into two subsets. Since the node  $u$  is the root, it uses the set of all vertices  $V$ , and generates two subsets  $S_{u,+}, S_{u,-}$  by partitioning  $V$ . Split-node  $v$  considers 3 subsets when searching for the optimal parameters to split on:  $V$  and the subsets generated by its ancestors; i.e.,  $S_{u,+}, S_{u,-}$ . It selects the parameters  $u, +$  and generates two subsets by partitioning its selected subset  $S_{u,+}$  into two new subsets:  $S_{v,+}$  and  $S_{v,-}$ . Node  $w$  considers 5 subsets:  $V$ , the two subsets generated in  $u$ ;  $S_{u,+}, S_{u,-}$ , and the two subsets generated in  $v$ ;  $S_{v,+}, S_{v,-}$ . Node  $w$  selects  $S_{v,-}$ .

The power of using dynamic features based on subsets is proved in Lemma 4.3. In particular, we show that if the walks are not restricted to subsets and the whole graph is always used, there are graphs with just 4 vertices that cannot be separated. This is in contrast to when subsets are used.

During learning we need to construct a DT where each split-node is defined via the parameters  $k, d, u, \rho, r$  (see Section 4 on the running time). This is explained next.

### 3.4 Learning TREE-Gs from Graph Data

During the training of standard decision trees, the tree is constructed in a greedy manner, where each split-node searches for the optimal feature to split on. In TREE-G, the tree is similarly constructed in a greedy manner, where each split-node searches for the optimal dynamic feature to split on, over all the dynamic features available to it. Each dynamic feature corresponds to a set of parameters  $k, d, u, \rho, r$ , and the selection of which dynamic feature to use is equivalent to searching over all the allowed combinations of these parameters. Finally, each split-node in the learned TREE-G is represented by the selected parameters. For practical reasons, it helps to bound the value of  $d$ . Bounding the search space for the pointer  $u$  can also improve efficiency. In particular, it is possible to limit every split-node to consider only ancestors at limited distance  $a$  from it. Note that in this case, every split-node still considers the set of all vertices  $V$ . Empirically, we found that bounding  $d \leq 2$  and  $a \leq 2$  suffices to achieve high performance, for the tasks we tested.

### 3.5 TREE-G for graph labeling

So far we have discussed TREE-G in the context of vertex labeling tasks. We now shift to graph labeling tasks in which a graph is given and its label needs to be predicted. While the general structure of TREE-G is preserved, some modifications are required.

In vertex labeling tasks the dynamic feature uses the  $i^{\text{th}}$  entry of the vector  $(A^d \circ M_r(S_{u,\rho})) \mathbf{f}_k$ , depending on the input vertex  $i$ . In graph labeling tasks, only the adjacency matrix  $A$  and the matrix of stacked feature vectors  $X$  are given, without a vertex  $i$ . To get a real value to compare against the threshold, we aggregate the vector  $(A^d \circ M_r(S_{u,\rho})) \mathbf{f}_k$  to a single value, using a permutation-invariant function. Now,  $\phi$  is parameterized by another parameter  $AGG$ , that indicates the aggregation function from among *sum*, *mean*, *min*, *max*. A dynamic feature in graph labeling tasks is computed as follows:

$$\phi_{k,d,u,\rho,r,AGG}(A, X) = AGG \left( (A^d \circ M_r(S_{u,\rho})) \mathbf{f}_k \right)$$

In graph labeling tasks, two additional walk types are used:

3. **Target Walks:** Only consider walks ending in the vertices in  $S$ .
4. **Target-Source Walks:** Only consider walks starting and ending in vertices of  $S$ .

Therefore the parameter  $r$  can take a value 3 for target walks or 4 for target-source walks. Similarly to types 1 and 2, it is simple to restrict the walks by zeroing out parts of the walks matrix  $A^d$ , given a subset of the vertices  $S$ . For target walks, zero out the  $j^{\text{th}}$  row in  $A^d$ , for each vertex  $j \notin S$ . For target-source walks, zero out the  $j^{\text{th}}$  column and  $j^{\text{th}}$  row in  $A^d$ , for  $j \notin S$ . In the appendix we empirically show that each of the four walk types is valuable for some task.

Notice that target masking (including target-source) is not useful in the vertex labeling setting since in this setting only the  $i^{\text{th}}$  coordinate of the vector  $(A^d \circ M_r(S_{u,\rho})) \mathbf{f}_k$  is used when making predictions for the  $i^{\text{th}}$  vertex. However, in the graph labeling, predictions are made for the entire graph and therefore use the entire vector.

Masking types that include zeroing out rows, eventually zero out entries in the vector  $(A^d \circ M_r(S_{u,\rho})) \mathbf{f}_k$ . As in graph labeling tasks this vector is aggregated, zeros may affect the results of some aggregations e.g. *min*. Therefore, in the case of target, target-source and cycle walks, the aggregation is only performed on the entries that are in the selected subset  $S_{u,\rho}$ ; i.e.,

$$AGG \left( ((A^d \circ M_r(S_{u,\rho})) \mathbf{f}_k)_{S_{u,\rho}} \right)$$

As in the vertex-labeling setting, once a dynamic feature is selected at a split-node, two subsets of the vertices are generated to be used by the descendant split-nodes in the tree, using the same definitions as in vertex labeling. In particular, the chosen aggregation is not part of the generation of the subsets. An exception is made when the selected aggregation function in the split-node is *sum*, in which case the subsets are defined with respect to a scaled threshold  $\theta/|S_{u,\rho}|$  instead of  $\theta$ . This is because in this case any value that is greater than this scaled threshold contributes towards satisfying the split criterion. In the Appendix we give a visual example of a trained TREE-G over a real-world dataset.

In the description above we described the way a single TREE-G is learned and used. However, multiple TREE-Gs can be used to form ensembles using Gradient Boosted Trees [46], Random Forests [5], or any other ensemble learning method.

## 4 Theoretical Properties of TREE-G

In this section we discuss some theoretical properties of TREE-G, including its computational complexity. Due to space limitation proofs are deferred to the Appendix. We first consider the invariance properties of TREE-G. Recall that a graph is described by its features  $\mathbf{f}_1, \mathbf{f}_2, \dots, \mathbf{f}_l$  and adjacency matrix  $A$ . If we apply a permutation  $P$  to the vertices we obtain a new adjacency matrix  $PAP^T$  and features  $P\mathbf{f}_k$ . Clearly, we would like a model that acts on graphs to provide the same output for the original and permuted graphs. In graph labeling tasks this means we would like the output of TREE-G to be invariant to  $P$ . In the case of vertex prediction, we expect equivariance such that if the graph is permuted with  $P$  then the prediction for the vertex  $\pi(i)$  would be the same as the

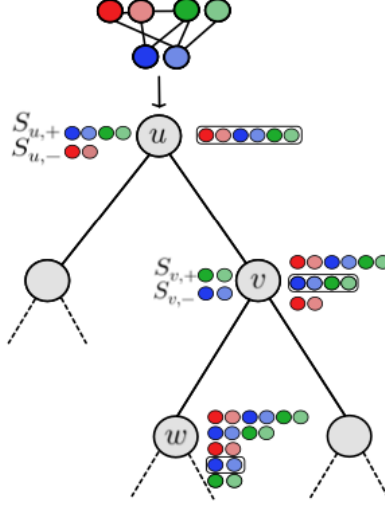


Figure 1: Example of the subsets generated in every split-node of the tree. After choosing the optimal parameters, two subsets are generated by partitioning the selected subset into two subsets. To the right of each split-node are the subsets considered in that split-node, where the selected subset is marked with a rectangle. To the left of each split-node are the generated subsets, which are a partition of the selected subset into two subsets.

prediction for the vertex  $i$  in the original graph [47]. The next lemma shows that this is the case for TREE-G.

**Lemma 4.1.** *TREE-G is invariant to permutations in the case of graph labeling and equivariant in the case of vertex labeling.*

To prove Lemma 4.1, we show that all TREE-G’s components are either invariant or equivariant under permutation of the vertices. The proof can be found in the Appendix, as all other proofs.

When training a decision tree, most of the computational effort is in searching the optimal feature to split on, at every split-node. The cost of this operation is proportional to the number of input features. In TREE-G, if features were to be generated for every subset of the vertices then the computation time would have been exponential in the graph size. Nevertheless, due to its dynamic mechanism where the subsets are computed incrementally in every split-node and not in advance (i.e. before seeing the graph and the tree), TREE-G is capable of searching over exponentially many dynamic features, corresponding to subsets of the vertices, without incurring the costs associated with it. Therefore, in TREE-G the running time of finding the optimal dynamic feature to split on, is also proportional to the number of input features.

**Lemma 4.2.** *The running time of searching for the optimal split in TREE-G is linear in the input features.*

Next, we present results on the expressive power of TREE-G. As mentioned above, the advantage of TREE-G lies in its ability to focus on subsets. We prove that TREE-G is strictly more expressive than a limited version of it where subsets are not used (equivalently, the used subset is always  $V$ ).

**Lemma 4.3.** *There exist graphs that are separable by TREE-G, but are inseparable if TREE-G is limited to not use subsets.*

Notice that standard decision trees that only act on the input features, are a special case of such limited TREE-G, where additionally the propagation depth is limited to 0. Therefore, an immediate conclusion is that TREE-G is strictly more expressive than these standard trees.

Finally, the following lemma shows that TREE-G can express classification rules that GNNs cannot.

**Lemma 4.4.** *There exist graphs that cannot be separated by GNNs but can be separated by TREE-G.*

This Lemma proves that there exist two graphs such that any GNN will assign both graphs with the same label, whereas there exists a TREE-G that will assign a different label to each graph. It was shown

Table 1: Empirical comparison of graph classification tasks. Best accuracy is highlighted in bold.

Baseline	PROT	MUTAG	D&D	IMDB-B	NCI1	PTC	IMDB-M	Mutagen	ENZ	HIV
XGraphBoost	67.0 $\pm$ 2.5	86.1 $\pm$ 3.8	72.9 $\pm$ 2.0	56.1 $\pm$ 1.4	61.9 $\pm$ 7.1	51.3 $\pm$ 5.0	41.5 $\pm$ 0.9	71.2 $\pm$ 2.5	58.5 $\pm$ 1.0	60.1 $\pm$ 5.3
BGNN	70.5 $\pm$ 2.4	80.2 $\pm$ 0.5	71.2 $\pm$ 0.9	68.0 $\pm$ 1.5	70.5 $\pm$ 2.0	55.5 $\pm$ 0.3	46.2 $\pm$ 2.3	65.0 $\pm$ 0.9	58.1 $\pm$ 1.5	77.0 $\pm$ 6.1
RW	72.5 $\pm$ 0.9	85.0 $\pm$ 4.5	70.0 $\pm$ 5.0	65.0 $\pm$ 1.2	69.0 $\pm$ 0.5	57.2 $\pm$ 1.0	45.1 $\pm$ 0.9	74.5 $\pm$ 0.5	55.1 $\pm$ 1.3	76.7 $\pm$ 2.1
WL	74.0 $\pm$ 3.0	82.0 $\pm$ 0.2	76.1 $\pm$ 3.0	72.8 $\pm$ 1.9	75.9 $\pm$ 1.0	58.9 $\pm$ 4.2	50.9 $\pm$ 3.8	73.4 $\pm$ 0.4	52.1 $\pm$ 3.0	75.7 $\pm$ 0.8
GAT	70.0 $\pm$ 1.9	84.4 $\pm$ 0.6	74.4 $\pm$ 0.3	70.6 $\pm$ 3.2	74.9 $\pm$ 0.1	56.2 $\pm$ 7.3	47.0 $\pm$ 1.9	72.2 $\pm$ 1.8	58.5 $\pm$ 1.2	<b>82.4 <math>\pm</math> 3.6</b>
GCN	73.2 $\pm$ 1.0	84.6 $\pm$ 0.7	71.2 $\pm$ 2.0	69.4 $\pm$ 1.9	76.0 $\pm$ 0.9	59.4 $\pm$ 10.3	50.0 $\pm$ 3.0	69.9 $\pm$ 1.5	<b>60.1 <math>\pm</math> 3.0</b>	76.6 $\pm$ 0.0
GraphSAGE	70.4 $\pm$ 2.0	86.1 $\pm$ 0.7	72.7 $\pm$ 1.0	69.9 $\pm$ 4.4	76.1 $\pm$ 2.2	<b>67.1 <math>\pm</math> 12.6</b>	47.8 $\pm$ 1.9	64.1 $\pm$ 0.3	58.2 $\pm$ 5.9	79.2 $\pm$ 1.2
GIN	72.2 $\pm$ 1.9	84.5 $\pm$ 0.8	75.2 $\pm$ 2.9	71.2 $\pm$ 3.4	<b>79.1 <math>\pm</math> 1.4</b>	55.6 $\pm$ 11.1	48.8 $\pm$ 5.0	69.4 $\pm$ 1.2	59.5 $\pm$ 0.2	77.8 $\pm$ 1.3
TREE-G (d=0,a=0) + TopFeatures	70.7 $\pm$ 0.9	86.1 $\pm$ 6.1	74.3 $\pm$ 3.0	61.0 $\pm$ 5.3	69.9 $\pm$ 3.0	53.0 $\pm$ 0.9	43.3 $\pm$ 1.2	73.4 $\pm$ 2.0	59.1 $\pm$ 1.0	70.3 $\pm$ 1.5
TREE-G (d=0,a=0)	73.4 $\pm$ 0.9	86.1 $\pm$ 6.0	74.4 $\pm$ 4.7	72.6 $\pm$ 2.4	70.4 $\pm$ 0.7	54.0 $\pm$ 0.5	52.3 $\pm$ 1.5	72.5 $\pm$ 2.2	58.1 $\pm$ 1.4	70.0 $\pm$ 0.8
TREE-G (a=0)	74.7 $\pm$ 0.9	89.3 $\pm$ 7.6	76.0 $\pm$ 4.5	72.5 $\pm$ 2.7	73.6 $\pm$ 2.2	59.0 $\pm$ 0.8	52.7 $\pm$ 1.5	72.6 $\pm$ 2.1	58.1 $\pm$ 3.9	78.1 $\pm$ 0.9
<b>TREE-G</b>	<b>75.6 <math>\pm</math> 1.1</b>	<b>91.0 <math>\pm</math> 5.7</b>	<b>76.2 <math>\pm</math> 4.5</b>	<b>73.0 <math>\pm</math> 2.4</b>	74.9 $\pm$ 2.1	59.1 $\pm$ 0.7	<b>56.4 <math>\pm</math> 0.9</b>	<b>76.7 <math>\pm</math> 0.2</b>	59.6 $\pm$ 0.9	81.8 $\pm$ 3.4

Table 2: Empirical comparison of node classification tasks. Best accuracy is highlighted in bold.

Baseline	CORA	CITeseer	PUBMED	ARXIV
XGraphBoost	60.5 $\pm$ 3.0	50.5 $\pm$ 3.4	61.9 $\pm$ 2.2	65.8 $\pm$ 1.9
BGNN	71.2 $\pm$ 5.0	69.1 $\pm$ 3.9	59.9 $\pm$ 0.1	67.0 $\pm$ 0.1
GAT	83.0 $\pm$ 0.6	70.0 $\pm$ 1.5	<b>79.1 <math>\pm</math> 0.7</b>	73.6 $\pm$ 0.1
GCN	81.0 $\pm$ 0.8	72.1 $\pm$ 0.3	79.0 $\pm$ 0.8	71.7 $\pm$ 0.2
GraphSAGE	81.4 $\pm$ 0.7	73.4 $\pm$ 0.8	78.4 $\pm$ 0.4	71.7 $\pm$ 0.2
GIN	80.0 $\pm$ 1.2	<b>75.1 <math>\pm</math> 1.9</b>	75.3 $\pm$ 0.9	<b>73.8 <math>\pm</math> 1.4</b>
TREE-G (d=0,a=0)	80.1 $\pm$ 1.0	70.2 $\pm$ 2.0	74.0 $\pm$ 0.5	67.1 $\pm$ 1.5
TREE-G (a=0)	80.3 $\pm$ 0.9	74.1 $\pm$ 1.2	72.9 $\pm$ 1.6	67.5 $\pm$ 0.6
<b>TREE-G</b>	<b>83.5 <math>\pm</math> 1.5</b>	74.1 $\pm$ 0.9	78.0 $\pm$ 3.1	73.4 $\pm$ 0.9

in [27, 48] that the expressive power of GNNs is bounded by the expressive power of the 1-WL test. Therefore, a direct conclusion of Theorem 4.4 is that the expressive power of TREE-G is different from the 1-WL class.

## 5 Empirical Evaluation

In what follows we report experiments on graph and vertex labeling benchmarks. We compare TREE-G to popular GNNs, graph kernels, and other tree-based methods.<sup>7</sup>

### 5.1 Datasets

**Graph Classification** We used nine graph classification benchmarks from TUDatasets [49], and one large-scale dataset from OGB [50]. **IMDB-B & IMDB-M** [51] are movie collaboration datasets, where each graph is labels with a genre. **MUTAG**, **NCI1**, **PROT**, **DD**, **ENZ**, **Mutagen** & **PTC** [18, 52, 53] are datasets of chemical compounds. In each dataset, the goal is to classify the compounds according to some property of interest. **HIV** [50] is a large-scale dataset of molecules that may inhibit HIV.

**Node Classification** We used the three datasets from Planetoid [54], and one large-scale dataset from OGB [50]: **Cora**, **Citeseer** and **Pubmed** are citation graphs, and **Arxiv** is a large-scale graph over 169343 nodes, representing the citation network between all Computer Science arXiv papers. More details on all datasets are given in the Appendix.

<sup>7</sup>Code is available at <https://github.com/TAU-MLwell/GTA---Graph-Trees-with-Attention>.



## 5.2 Baselines

We compare TREE-G to six popular graph kernels and GNNs baselines: Graph Convolution Network (GCN) [17], Graph Attention Network (GAT) [16], GraphSAGE [55], Graph Isomorphism Network (GIN) [27], Weisfeiler-Lehman Graph kernels (WL) [18] and a Random-Walk kernels (RW) [25]. We also compared to the two methods combining GNNs and DTs described in Section 2: BGNN [44] and XGraphBoost [41].

Additionally, we report two ablations of TREE-G where we do not use the topology of the graph and/or the only used subset is the set of all vertices. This is done by limiting the propagation depth to 0 and/or the distance of the ancestors from which to consider subsets from, to 0. In TREE-G ( $a = 0$ ) we always use the whole graph as the selected subset. In TREE-G ( $d = 0, a = 0$ ) we do not use the topology of the graph (i.e. we always use  $A^0$ ) and we always use the whole graph as the selected subset. Notice TREE-G ( $d = 0, a = 0$ ) is equivalent to standard trees that only act on the input features. Finally, in TREE-G ( $d = 0, a = 0 + \text{TopFeatures}$ ) we evaluated the TREE-G equivalence to standard trees, with 8 additional topology-based features that are extracted from the graph in advance. As common in the literature [56, 57], we used 3 graph-level features: the dimension of the null space, the spectral gap (the smallest non-zero eigen-value), the second smallest eigenvalue (the algebraic connectivity). As vertex-level features, we added: the local clustering coefficient, the harmonic centrality, the rank according to the pagerank algorithm, and the hubs and authorities according to the HITS algorithm, to each vertex.

We used TREE-G in a GBT framework, with 50 TREE-G estimators. To improve the running time and reduce overfitting, we did not use all the walk types during training. Instead, we sampled each walk type with a fixed probability  $p \in [0, 1]$ , in every split-node. If the sampling ended with no types, no subsets are used (i.e. the set  $V$  is always used). We used  $p = 0.25$  for graph labeling tasks and  $p = 0.5$  for vertex labeling tasks. Following the protocol in [27], for all graph-classification except *HIV*, we report the best accuracy over 10-fold cross validation. As an alternative evaluation method, we also report 10-fold nested cross validation accuracy in the Appendix. Following [16, 17, 55], for the node-classification datasets we tuned the parameters on the Cora dataset using the pre-defined splits from [17]. We report the test accuracies averaged over 10 runs, using the parameters obtained from the best accuracy on the validation set. For the OGB datasets (*HIV* and *ARXIV*) we followed the protocols in Hu et al. [50], and used the predefined splits defined in the data, for tuning and testing (see the Appendix for more details). We used a 3rd party library<sup>8</sup> for the GBT framework, with its default parameters. The only parameters we tuned are the bound of the propagation depth  $d \in \{0, 1, 2\}$  and the maximal distance of ancestor from which to consider subsets  $a \in \{0, 1, 2\}$ . In all the experiments we added the constant feature 1 to all the vertices, to allow the models to compute features such as the vertex degree.

## 5.3 Results

The results are summarized in Table 1 and Table 2. TREE-G outperformed all other tree-based approaches (XGraphBoost, BGNN, TREE-G ( $d = 0, a = 0$ ), TREE-G ( $a = 0$ ), TREE-G ( $d = 0, a = 0 + \text{TopFeatures}$ )) on all 14 tasks. It outperformed graph-kernels in 9 out of the 10 graph classification tasks, and outperformed GNNs in 6 out of these 10 tasks. Specifically, TREE-G improved upon GNN approaches by a margin greater than 6.4 percentage points on the IMDB-M dataset and a margin greater than 4.9 and 2.4 percentage points on MUTAG and PROTEINS datasets, respectively. Regarding the vertex classification datasets, TREE-G outperformed most GNNs, and was on par with the leading GNN approach in every task. Note that TREE-G always outperformed TREE-G ( $a = 0$ ), which indicates that the use of subsets leads to improved performance. Our results demonstrate that methods that are fully based on decision trees, when specialized for graphs, are competitive with, and even outperform, popular GNNs and graph kernels.

## 6 Explaining TREE-G Outputs

This section discusses examples of the explanation mechanism of TREE-G. Following [45], the explanation mechanism ranks the vertices of the graph according to their presence in selected subsets and thus highlights the parts of the graph that contribute the most to the prediction. Due to space

<sup>8</sup><https://maxhalford.github.io/starboost/>

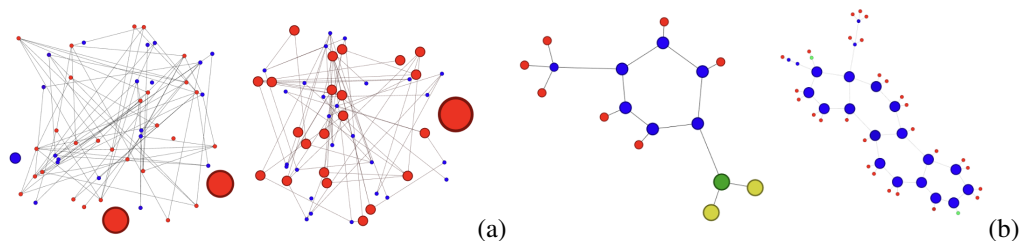


Figure 2: Vertex-level explanations for two graphs from the Red Isolated Vertex problem (a) and two graphs from the Mutagenicity problem (b). The size of vertices corresponds to their importance according to the explanations mechanism. The importance score uses the selected subsets in the trees.

limitations, we defer the formulation of the ranking to the Appendix, together with an explanation mechanism for edges, which ranks the edges of the graph. As is the case in most tree methods, dynamic features do not combine multiple features, which makes them more interpretable and less prone to overfitting. We present examples of vertex explanations for two problems: Red Isolated Vertex, and Mutagenicity.

**Red-Isolated-Node Explanations:** This is a synthetic task to determine whether exactly one red vertex is isolated in the graph. The data consists of 1000 graphs with 50 vertices each, with two features: the constant feature 1 and a binary blue/red color.

**Mutagenicity Explanations:** We used the Mutagen dataset described in Section 5, where the goal is to classify chemical compounds into mutagen and non-mutagen.

For each task, we trained and tested GBT with 50 TREE-G estimators. We limited the propagation depth to 2 and the distance of the ancestors from which to consider subsets, to 2 as well. We used a 80/20 random train-test splits. Figures 2a and 2b present vertex explanations for two graphs from the test sets of the Red-Isolated-Node experiments and the Mutagenicity experiments, respectively. The size of a vertex corresponds to its importance computed by the explanations mechanism. For the Red-Isolated-Node problem, it is shown that TREE-G attended to isolated vertices, and even more so to red isolated vertices. For the Mutagenicity problem, TREE-G attended to  $NO_2$  (green and yellow subgraph) and carbon-rings (blue cycles), which are known to have mutagenic effects [24].

## 7 Conclusion

Graphs arise in many important applications of machine learning. In this work we proposed a novel method, Decision Trees with Dynamic Graph Features (TREE-G), to perform different prediction tasks on graphs, inspired by the success of tree-based methods on tabular data [1–3]. Empirically we showed that TREE-G outperforms other tree-based models that were adapted to operate on graphs. Moreover, when compared to commonly used Graph Neural Networks (GNNs) and graph kernels, we found that TREE-G was on par in all cases and outperformed all other methods in many benchmarks. Our theoretical analysis showed that the dynamic features in TREE-G strictly improve its expressive power with respect to standard trees that only act on input features, even when those input features are extended with some topology-based features. We also showed that the expressive power of TREE-G is different from the expressive power of GNNs, as there are graphs that GNNs fail to tell apart, while TREE-G manages to separate them. Finally, we also proposed a mechanism for generating explanations for TREE-G decisions. The novel concept in TREE-G is to split the data on dynamic features that utilize properties of graphs and focus on substructures; however, it may be possible to adapt dynamic features to other types of data such as time-series, sequences, and tabular data.

## 8 Acknowledgments

This work has been supported by the Israeli Science Foundation research grant 1186/18

## References

- [1] Ravid Shwartz-Ziv and Amitai Armon. Tabular data: Deep learning is not all you need. In *8th ICML Workshop on Automated Machine Learning (AutoML)*, 2021. URL <https://openreview.net/forum?id=vdgtepS1pV>.
- [2] Te Han, Dongxiang Jiang, Qi Zhao, Lei Wang, and Kai Yin. Comparison of random forest, artificial neural networks and support vector machine for intelligent diagnosis of rotating machinery. *Transactions of the Institute of Measurement and Control*, 40(8):2681–2693, 2018. doi: 10.1177/0142331217708242. URL <https://doi.org/10.1177/0142331217708242>.
- [3] Yunus Miah, Chowdhury Prima, Sharmeen Seema, Mufti Mahmud, and M. Shamim Kaiser. *Performance Comparison of Machine Learning Techniques in Identifying Dementia from Open Access Clinical Datasets*, pages 79–89. 01 2021. ISBN 978-981-15-6047-7. doi: 10.1007/978-981-15-6048-4\_8.
- [4] Léo Grinsztajn, Edouard Oyallon, and Gaël Varoquaux. Why do tree-based models still outperform deep learning on tabular data?, 2022. URL <https://arxiv.org/abs/2207.08815>.
- [5] Tin Kam Ho. Random decision forests. In *Proceedings of 3rd international conference on document analysis and recognition*, volume 1, pages 278–282. IEEE, 1995.
- [6] Jerome H. Friedman. Greedy function approximation: A gradient boosting machine. *Annals of Statistics*, 29:1189–1232, 2000.
- [7] Jerome H. Friedman. Stochastic gradient boosting. *Comput. Stat. Data Anal.*, 38(4):367–378, feb 2002. ISSN 0167-9473. doi: 10.1016/S0167-9473(01)00065-2. URL [https://doi.org/10.1016/S0167-9473\(01\)00065-2](https://doi.org/10.1016/S0167-9473(01)00065-2).
- [8] Alessandro Sperduti and Antonina Starita. Supervised neural networks for the classification of structures. *IEEE Transactions on Neural Networks*, 8(3):714–735, 1997.
- [9] M. Gori, G. Monfardini, and F. Scarselli. A new model for learning in graph domains. In *Proceedings. 2005 IEEE International Joint Conference on Neural Networks, 2005.*, volume 2, pages 729–734 vol. 2, 2005. doi: 10.1109/IJCNN.2005.1555942.
- [10] Yujia Li, Daniel Tarlow, Marc Brockschmidt, and Richard Zemel. Gated graph sequence neural networks, 2017.
- [11] Will Hamilton, Zhitao Ying, and Jure Leskovec. Inductive representation learning on large graphs. In I. Guyon, U. V. Luxburg, S. Bengio, H. Wallach, R. Fergus, S. Vishwanathan, and R. Garnett, editors, *Advances in Neural Information Processing Systems*, volume 30. Curran Associates, Inc., 2017. URL <https://proceedings.neurips.cc/paper/2017/file/5dd9db5e033da9c6fb5ba83c7a7e9ea9-Paper.pdf>.
- [12] David Duvenaud, Dougal Maclaurin, Jorge Aguilera-Iparraguirre, Rafael Gómez-Bombarelli, Timothy Hirzel, Alán Aspuru-Guzik, and Ryan P. Adams. Convolutional networks on graphs for learning molecular fingerprints, 2015.
- [13] Michaël Defferrard, Xavier Bresson, and Pierre Vandergheynst. Convolutional neural networks on graphs with fast localized spectral filtering. In D. Lee, M. Sugiyama, U. Luxburg, I. Guyon, and R. Garnett, editors, *Advances in Neural Information Processing Systems*, volume 29. Curran Associates, Inc., 2016. URL <https://proceedings.neurips.cc/paper/2016/file/04df4d434d481c5bb723be1b6df1ee65-Paper.pdf>.
- [14] David G. T. Barrett, Felix Hill, Adam Santoro, Ari S. Morcos, and Timothy Lillicrap. Measuring abstract reasoning in neural networks, 2018.
- [15] Octavian-Eugen Ganea, Lagnajit Pattanaik, Connor W. Coley, Regina Barzilay, Klavs F. Jensen, William H. Green, and Tommi S. Jaakkola. Geomol: Torsional geometric generation of molecular 3d conformer ensembles, 2021.

- [16] Petar Veličković, Guillem Cucurull, Arantxa Casanova, Adriana Romero, Pietro Liò, and Yoshua Bengio. Graph attention networks. In *International Conference on Learning Representations*, 2018.
- [17] Thomas N. Kipf and Max Welling. Semi-supervised classification with graph convolutional networks, 2017.
- [18] Nino Shervashidze, Pascal Schweitzer, Erik Jan van Leeuwen, Kurt Mehlhorn, and Karsten M. Borgwardt. Weisfeiler-lehman graph kernels. *J. Mach. Learn. Res.*, 12:2539–2561, 2011. URL <http://dblp.uni-trier.de/db/journals/jmlr/jmlr12.html#ShervashidzeSLMB11>.
- [19] Nino Shervashidze, S. V. N. Vishwanathan, Tobias Petri, Kurt Mehlhorn, and Karsten M. Borgwardt. Efficient graphlet kernels for large graph comparison. *Journal of Machine Learning Research - Proceedings Track*, 5:488–495, 2009. URL <http://dblp.uni-trier.de/db/journals/jmlr/jmlrp5.html#ShervashidzeVPMB09>.
- [20] Emanuele Rossi, Ben Chamberlain, Fabrizio Frasca, Davide Eynard, Federico Monti, and Michael Bronstein. Temporal graph networks for deep learning on dynamic graphs, 2020.
- [21] John Ingraham, Vikas Garg, Regina Barzilay, and Tommi Jaakkola. Generative models for graph-based protein design. In H. Wallach, H. Larochelle, A. Beygelzimer, F. d’Alché-Buc, E. Fox, and R. Garnett, editors, *Advances in Neural Information Processing Systems*, volume 32. Curran Associates, Inc., 2019. URL <https://proceedings.neurips.cc/paper/2019/file/f3a4ff4839c56a5f460c88cce3666a2b-Paper.pdf>.
- [22] Ian Barnett, Nishant Malik, Marieke L Kuijjer, Peter J Mucha, and Jukka-Pekka Onnela. Feature-based classification of networks. *arXiv preprint arXiv:1610.05868*, 2016.
- [23] Nathan de Lara and Edouard Pineau. A simple baseline algorithm for graph classification. *arXiv preprint arXiv:1810.09155*, 2018.
- [24] AK Debnath, RL Lopez de Compadre, G Debnath, AJ Shusterman, and C Hansch. Structure-activity relationship of mutagenic aromatic and heteroaromatic nitro compounds. correlation with molecular orbital energies and hydrophobicity. *Journal of medicinal chemistry*, 34(2): 786–797, February 1991. ISSN 0022-2623. doi: 10.1021/jm00106a046. URL <https://doi.org/10.1021/jm00106a046>.
- [25] Thomas Gärtner, Peter Flach, and Stefan Wrobel. On graph kernels: Hardness results and efficient alternatives. In Bernhard Schölkopf and Manfred K. Warmuth, editors, *Computational Learning Theory and Kernel Machines — Proceedings of the 16th Annual Conference on Computational Learning Theory and 7th Kernel Workshop (COLT/Kernel 2003) August 24–27, 2003, Washington, DC, USA*, volume 2777 of *Lecture Notes in Computer Science*, pages 129–143. Springer, Berlin–Heidelberg, Germany, August 2003.
- [26] Muhan Zhang, Zhicheng Cui, Marion Neumann, and Yixin Chen. An end-to-end deep learning architecture for graph classification. In *AAAI*, 2018.
- [27] Keyulu Xu, Weihua Hu, Jure Leskovec, and Stefanie Jegelka. How powerful are graph neural networks? In *International Conference on Learning Representations*, 2019. URL <https://openreview.net/forum?id=ryGs6iA5Km>.
- [28] Yifan Feng, Haoxuan You, Zizhao Zhang, Rongrong Ji, and Yue Gao. Hypergraph neural networks. *Proceedings of the AAAI Conference on Artificial Intelligence*, 33(01):3558–3565, Jul. 2019. doi: 10.1609/aaai.v33i01.33013558. URL <https://ojs.aaai.org/index.php/AAAI/article/view/4235>.
- [29] Justin Gilmer, Samuel S. Schoenholz, Patrick F. Riley, Oriol Vinyals, and George E. Dahl. Neural message passing for quantum chemistry, 2017.
- [30] Marinka Zitnik, Monica Agrawal, and Jure Leskovec. Modeling polypharmacy side effects with graph convolutional networks. *Bioinformatics*, 34(13):i457–i466, 06 2018. ISSN 1367-4803. doi: 10.1093/bioinformatics/bty294. URL <https://doi.org/10.1093/bioinformatics/bty294>.

- [31] Rex Ying, Ruining He, Kaifeng Chen, Pong Eksombatchai, William L. Hamilton, and Jure Leskovec. Graph convolutional neural networks for web-scale recommender systems. *Proceedings of the 24th ACM SIGKDD International Conference on Knowledge Discovery & Data Mining*, Jul 2018. doi: 10.1145/3219819.3219890. URL <http://dx.doi.org/10.1145/3219819.3219890>.
- [32] Zonghan Wu, Shirui Pan, Fengwen Chen, Guodong Long, Chengqi Zhang, and S Yu Philip. A comprehensive survey on graph neural networks. *IEEE transactions on neural networks and learning systems*, 32(1):4–24, 2020.
- [33] Jie Zhou, Ganqu Cui, Shengding Hu, Zhengyan Zhang, Cheng Yang, Zhiyuan Liu, Lifeng Wang, Changcheng Li, and Maosong Sun. Graph neural networks: A review of methods and applications. *AI Open*, 1:57–81, 2020.
- [34] Giannis Nikolentzos, Giannis Siglidis, and Michalis Vazirgiannis. Graph kernels: A survey. *Journal of Artificial Intelligence Research*, 72:943–1027, nov 2021. doi: 10.1613/jair.1.13225. URL <https://doi.org/10.1613/jair.1.13225>.
- [35] Jeff Heaton. An empirical analysis of feature engineering for predictive modeling. In *Southeast-Con 2016*, pages 1–6. IEEE, 2016.
- [36] Tong He, Marten Heidemeyer, Fuqiang Ban, Artem Cherkasov, and Martin Ester. Simboost: a read-across approach for predicting drug–target binding affinities using gradient boosting machines. *Journal of cheminformatics*, 9(1):1–14, 2017.
- [37] Xiujuan Lei and Zengqiang Fang. Gbdtcda: predicting circrna-disease associations based on gradient boosting decision tree with multiple biological data fusion. *International journal of biological sciences*, 15(13):2911, 2019.
- [38] Mingcong Wu, Yong Huang, Liang Zhao, and Yue He. Link prediction based on random forest in signed social networks. In *2018 10th International Conference on Intelligent Human-Machine Systems and Cybernetics (IHMSC)*, volume 02, pages 251–256, 2018. doi: 10.1109/IHMSC.2018.10164.
- [39] Kuanyang Li and Lilan Tu. Link prediction for complex networks via random forest. *Journal of Physics: Conference Series*, 1302:022030, 08 2019. doi: 10.1088/1742-6596/1302/2/022030.
- [40] Pan Li, Zhen Qin, Xuanhui Wang, and Donald Metzler. Combining decision trees and neural networks for learning-to-rank in personal search. In *Proceedings of the 25th ACM SIGKDD International Conference on Knowledge Discovery & Data Mining, KDD '19*, page 2032–2040, New York, NY, USA, 2019. Association for Computing Machinery. ISBN 9781450362016. doi: 10.1145/3292500.3330676. URL <https://doi.org/10.1145/3292500.3330676>.
- [41] Daiguo Deng, Xiaowei Chen, Ruochi Zhang, Zengrong Lei, Xiaojian Wang, and Fengfeng Zhou. Xgraphboost: Extracting graph neural network-based features for a better prediction of molecular properties. *Journal of Chemical Information and Modeling*, 61(6):2697–2705, 2021. doi: 10.1021/acs.jcim.0c01489. URL <https://doi.org/10.1021/acs.jcim.0c01489>. PMID: 34009965.
- [42] Jonathan M. Stokes, Kevin Yang, Kyle Swanson, Wengong Jin, Andres Cubillos-Ruiz, Nina M. Donghia, Craig R. MacNair, Shawn French, Lindsey A. Carfrae, Zohar Bloom-Ackermann, Victoria M. Tran, Anush Chiappino-Pepe, Ahmed H. Badran, Ian W. Andrews, Emma J. Chory, George M. Church, Eric D. Brown, Tommi S. Jaakkola, Regina Barzilay, and James J. Collins. A deep learning approach to antibiotic discovery. *Cell*, 180(4):688–702.e13, 2020. ISSN 0092-8674. doi: <https://doi.org/10.1016/j.cell.2020.01.021>. URL <https://www.sciencedirect.com/science/article/pii/S0092867420301021>.
- [43] Rushabh Patel and Yanhui Guo. Graph based link prediction between human phenotypes and genes, 2021.
- [44] Sergei Ivanov and Liudmila Prokhorenkova. Boost then convolve: Gradient boosting meets graph neural networks, 2021.

- [45] Roy Hirsch and Ran Gilad-Bachrach. Trees with attention for set prediction tasks. In Marina Meila and Tong Zhang, editors, *Proceedings of the 38th International Conference on Machine Learning*, volume 139 of *Proceedings of Machine Learning Research*, pages 4250–4261. PMLR, 18–24 Jul 2021. URL <https://proceedings.mlr.press/v139/hirsch21a.html>.
- [46] Jerome H Friedman. Greedy function approximation: a gradient boosting machine. *Annals of statistics*, pages 1189–1232, 2001.
- [47] Justin Gilmer, Samuel S. Schoenholz, Patrick F. Riley, Oriol Vinyals, and George E. Dahl. Neural message passing for quantum chemistry, 2017. URL <https://arxiv.org/abs/1704.01212>.
- [48] Vikas K. Garg, Stefanie Jegelka, and Tommi Jaakkola. Generalization and representational limits of graph neural networks, 2020.
- [49] Christopher Morris, Nils M. Kriege, Franka Bause, Kristian Kersting, Petra Mutzel, and Marion Neumann. Tudataset: A collection of benchmark datasets for learning with graphs. In *ICML 2020 Workshop on Graph Representation Learning and Beyond (GRL+ 2020)*, 2020. URL [www.graphlearning.io](http://www.graphlearning.io).
- [50] Weihua Hu, Matthias Fey, Marinka Zitnik, Yuxiao Dong, Hongyu Ren, Bowen Liu, Michele Catasta, and Jure Leskovec. Open graph benchmark: Datasets for machine learning on graphs, 2020. URL <https://arxiv.org/abs/2005.00687>.
- [51] Pinar Yanardag and S.V.N. Vishwanathan. Deep graph kernels. In *Proceedings of the 21th ACM SIGKDD International Conference on Knowledge Discovery and Data Mining, KDD '15*, page 1365–1374, New York, NY, USA, 2015. Association for Computing Machinery. ISBN 9781450336642. doi: 10.1145/2783258.2783417. URL <https://doi.org/10.1145/2783258.2783417>.
- [52] Nils Kriege and Petra Mutzel. Subgraph matching kernels for attributed graphs. In *Proceedings of the 29th International Conference on Machine Learning, ICML 12*, page 291–298, Madison, WI, USA, 2012. Omnipress. ISBN 9781450312851.
- [53] Kaspar Riesen and Horst Bunke. Iam graph database repository for graph based pattern recognition and machine learning. In Niels da Vitoria Lobo, Takis Kasparis, Fabio Roli, James T. Kwok, Michael Georgiopoulos, Georgios C. Anagnostopoulos, and Marco Loog, editors, *Structural, Syntactic, and Statistical Pattern Recognition*, pages 287–297, Berlin, Heidelberg, 2008. Springer Berlin Heidelberg. ISBN 978-3-540-89689-0.
- [54] Zhilin Yang, William W. Cohen, and Ruslan Salakhutdinov. Revisiting semi-supervised learning with graph embeddings, 2016. URL <https://arxiv.org/abs/1603.08861>.
- [55] William L. Hamilton, Rex Ying, and Jure Leskovec. Inductive representation learning on large graphs, 2018.
- [56] Nathan de Lara and Edouard Pineau. A simple baseline algorithm for graph classification, 2018. URL <https://arxiv.org/abs/1810.09155>.
- [57] Peng Li, Kong Fanrang, Qingbo He, and Yongbin Liu. Multiscale slope feature extraction for rotating machinery fault diagnosis using wavelet analysis. *Measurement*, 46:497–505, 01 2013. doi: 10.1016/j.measurement.2012.08.007.
- [58] AK Debnath, RL Lopez de Compadre, G Debnath, AJ Shusterman, and C Hansch. Structure-activity relationship of mutagenic aromatic and heteroaromatic nitro compounds. correlation with molecular orbital energies and hydrophobicity. *Journal of medicinal chemistry*, 34(2): 786–797, February 1991. ISSN 0022-2623. doi: 10.1021/jm00106a046. URL <https://doi.org/10.1021/jm00106a046>.
- [59] Paul D. Dobson and Andrew J. Doig. Distinguishing enzyme structures from non-enzymes without alignments. *Journal of molecular biology*, 330 4:771–83, 2003.
- [60] Frank Harary and R. Z. Norman. Some properties of line digraphs. *Rendiconti del Circolo Matematico di Palermo*, 9:161–168, 1960.

- [61] Jiaxuan You, Jonathan Gomes-Selman, Rex Ying, and Jure Leskovec. Identity-aware graph neural networks, 2021. URL <https://arxiv.org/abs/2101.10320>.
- [62] K. V. Rashmi and Ran Gilad-Bachrach. Dart: Dropouts meet multiple additive regression trees, 2015.

## A Appendix A

In the appendix we present supporting material that did not fit in the main paper due to space limitations.

### A.1 Datasets Summary

Table 3 presents a summary of the datasets used in the experiments. The datasets used vary in the number of graphs, the sizes of the graphs, the number of features in each vertex and the number of classes. Note that although all benchmarks are classification tasks, TREE-G can also perform regression tasks, ranking tasks and more.

Table 3: Statistics of datasets used in experiments.

Dataset	# Graphs	Avg # Vertices	Avg # Edges	# Features	# Classes
PROT[49]	1113	39.06	72.82	3	2
MUTAG[49]	188	17.93	19.79	7	2
DD [49]	1178	284.32	715.66	0	2
IMDB-B [49]	1000	19	96	0	2
NCII[49]	4110	29.87	32.3	37	2
PTC[49]	344	14	14	19	2
IMDB-M [49]	1500	13	65	0	3
Mutagen [49]	4337	30.32	30.37	7	2
ENZ [49]	600	32.63	62.14	3	6
HIV[50]	41,127	25.5	27.5	9	2

Dataset	# Vertices	# Edges	# Features	# Classes
CORA[54]	2,708	10,556	1,433	7
CITeseer[54]	3,327	9,104	3,703	6
PUBMED[54]	19,717	88,648	500	3
ARXIV[50]	169,343	1,166,243	128	40

**MUTAG** [58] is a dataset of 188 chemical compounds divided into two classes according to their mutagenic effect on bacterium. **IMDB-B & IMDB-M** [51] are movie collaboration datasets with 1000 and 1500 graphs respectively. Each graph is derived from a genre, and the task is to predict this genre from the graph. Nodes represents actors/actresses and edges connect them if they have appeared in the same movie. **PROT, DD & ENZ** [18, 59] are datasets of chemical compounds consisting of 1113 and 1178 and 600 graphs, respectively. The goal in the first two datasets is to predict whether a compound is an enzyme or not, and the goal in the last datasets is to classify the type of an enzyme among 6 classes. **NCII** [18] is a datasets consisting of 4110 graphs, representing chemical compounds. Vertices and edges represents atoms and chemical bonds between them. The graphs are divided into two classes according to their ability to suppress or inhibit tumor growth. **Mutageny** [53] is a datasets consisting of 4337 chemical compounds of drugs divided into two classes: mutagen and non-mutagen. A mutagen is a compound that changes genetic material such as DNA, and increases mutation frequency. **PTC** [52] is a dataset consisting of 344 chemical compounds divided into two classes according to their carcinogenicity for rats. **HIV** [50] is a large-scale dataset consisting of 166k molecules and the task is to predict whether a molecule inhibits HIV.

**Node Classification** As node classification tasks, we used the three Planetoid datasets [54], and one large-scale dataset from OGB [50]: **Cora, Citeseer and Pubmed** are citation graphs consisting of 2708, 3327 and 19717 nodes respectively, where nodes are documents and edges are citation links. **Arxiv** is a large-scale directed graph over 169343 nodes, representing the citation network between all Computer Science (CS) arXiv papers.

### A.2 Additional Experiments Details and Results

In this section we describe additional details about the experiments whose results were reported in the main paper. The HIV and ARXIV datasets are large-scale datasets provided in the Open Graph Benchmark (OGB) paper [50] with pre-defined train and test splits and different metrics and protocols



Table 4: Empirical comparison of graph classification tasks, evaluated with nested cross validation. Best accuracy is highlighted in bold.

Baseline	PROT	MUTAG	D&D	IMDB-B	NCII	PTC	IMDB-M	Mutagen	ENZ	HIV
XGraphBoost	65.0 $\pm$ 1.2	86.0 $\pm$ 4.1	71.5 $\pm$ 1.0	57.0 $\pm$ 0.5	61.1 $\pm$ 5.0	50.2 $\pm$ 5.0	41.5 $\pm$ 0.9	71.2 $\pm$ 2.5	59.0 $\pm$ 1.4	
BGNN	70.2 $\pm$ 3.5	81.0 $\pm$ 0.9	70.5 $\pm$ 1.3	69.1 $\pm$ 1.4	72.0 $\pm$ 1.8	57.0 $\pm$ 2.1	45.9 $\pm$ 1.4	65.0 $\pm$ 3.0	57.2 $\pm$ 2.5	
RW	72.2 $\pm$ 1.5	84.8 $\pm$ 2.9	70.6 $\pm$ 4.1	65.1 $\pm$ 2.0	69.7 $\pm$ 1.0	57.0 $\pm$ 1.1	45.0 $\pm$ 1.0	72.2 $\pm$ 1.5	55.7 $\pm$ 1.9	
WL	74.1 $\pm$ 2.0	82.5 $\pm$ 2.0	75.9 $\pm$ 1.6	72.0 $\pm$ 2.0	74.8 $\pm$ 0.5	59.2 $\pm$ 3.1	51.6 $\pm$ 2.1	73.5 $\pm$ 0.2	54.0 $\pm$ 1.9	
GAT	70.2 $\pm$ 1.3	84.0 $\pm$ 0.9	74.1 $\pm$ 1.5	71.2 $\pm$ 3.0	75.0 $\pm$ 0.4	55.9 $\pm$ 6.0	46.5 $\pm$ 1.2	71.0 $\pm$ 1.9	58.7 $\pm$ 1.5	
GCN	72.9 $\pm$ 2.0	85.0 $\pm$ 0.9	71.0 $\pm$ 1.5	68.5 $\pm$ 1.0	75.8 $\pm$ 0.4	59.1 $\pm$ 6.9	50.3 $\pm$ 1.4	70.5 $\pm$ 0.7	60.5 $\pm$ 1.2	
GraphSAGE	71.2 $\pm$ 1.5	85.9 $\pm$ 1.0	71.8 $\pm$ 2.3	69.0 $\pm$ 1.6	75.8 $\pm$ 1.6	<b>67.3 <math>\pm</math> 1.4</b>	45.6 $\pm$ 0.3	62.0 $\pm$ 0.9	57.5 $\pm$ 2.4	
GIN	72.9 $\pm$ 0.5	83.0 $\pm$ 0.4	75.1 $\pm$ 1.3	72.0 $\pm$ 1.9	<b>79.3 <math>\pm</math> 1.2</b>	55.2 $\pm$ 5.7	48.5 $\pm$ 2.1	68.5 $\pm$ 2.0	59.9 $\pm$ 0.1	
TREE-G (d=0,a=0) + TopFeatures	68.5 $\pm$ 0.5	86.0 $\pm$ 3.9	73.2 $\pm$ 1.9	61.3 $\pm$ 5.0	68.2 $\pm$ 1.5	51.4 $\pm$ 2.5	43.8 $\pm$ 2.0	73.5 $\pm$ 1.8	58.8 $\pm$ 0.6	
TREE-G (d=0,a=0)	74.0 $\pm$ 0.8	86.2 $\pm$ 5.5	74.0 $\pm$ 3.4	71.6 $\pm$ 1.3	70.9 $\pm$ 0.5	52.1 $\pm$ 0.9	53.7 $\pm$ 1.1	72.4 $\pm$ 1.7	57.2 $\pm$ 2.5	
TREE-G (a=0)	75.2 $\pm$ 1.2	88.4 $\pm$ 2.7	75.0 $\pm$ 2.9	72.6 $\pm$ 1.0	73.2 $\pm$ 1.7	59.2 $\pm$ 1.5	52.5 $\pm$ 1.2	71.9 $\pm$ 3.0	58.5 $\pm$ 3.0	
<b>TREE-G</b>	<b>75.4 <math>\pm</math> 2.0</b>	<b>90.5 <math>\pm</math> 3.5</b>	<b>76.0 <math>\pm</math> 3.4</b>	<b>73.1 <math>\pm</math> 2.1</b>	75.7 $\pm$ 3.0	58.5 $\pm$ 0.9	<b>56.1 <math>\pm</math> 1.0</b>	<b>73.9 <math>\pm</math> 0.5</b>	<b>60.8 <math>\pm</math> 1.5</b>	

for each dataset. As common in the literature when evaluating OGB datasets, for each of these two datasets we follow its defined metric and protocol:

- In the case of the HIV dataset, the used metric is ROC-AUC. As described in Hu et al. [50], we ran the TREE-G 10 times and reported the mean ROC-AUC and std over the runs.
- In the case of the ARXIV dataset, the metric used is accuracy. Following the protocol in Hu et al. [50], we ran TREE-G 10 times and reported the mean accuracy and std over the runs.

For multi-class tasks we train TREE-G in a one-vs-all approach.

We also provide the results of 9 graph-level datasets that were evaluated with cross-validation, when evaluated with nested cross-validation. We used the same 10 folds for the outer loop and 5 folds for the inner loop.

### A.3 Extensions to TREE-G

In this section we propose some possible extensions to the TREE-G.

#### A.3.1 Weighted Adjacencies and Multiple Graphs

We note that the adjacency matrix used in TREE-G can be weighted. Moreover, it is possible to extend TREE-G to allow multiple adjacency matrices. This allows, for example, encoding of edge features and heterogeneous graphs.

#### A.3.2 Edge Level Tasks

In the paper we discuss vertex and graph level tasks. Nevertheless edge-level tasks also arise in many problems.

We note that the task of edge labeling can be represented as a vertex-level task by using a line graph [60]. The line graph  $L(G)$  of a graph  $G = (V, E)$  represents the adjacencies between the edges of  $G$ . Each edge  $(u, v) \in E$  corresponds to a vertex in  $L(G)$ , and two vertices in  $L(G)$  are connected by an edge if their corresponding edges in  $G$  share a vertex. Then, TREE-G for vertex-level tasks can be used to label vertices in the line graph, which corresponds to edges in the original graph.

### A.4 Example of a TREE-G Tree on Real Data

Figure 3 presents one TREE-G tree in the ensemble of the MUTAG experiment presented in the experiments section. The MUTAG dataset contains 188 chemical compounds divided into two classes according to their mutagenic effect on bacterium. Each node is associated with one feature in

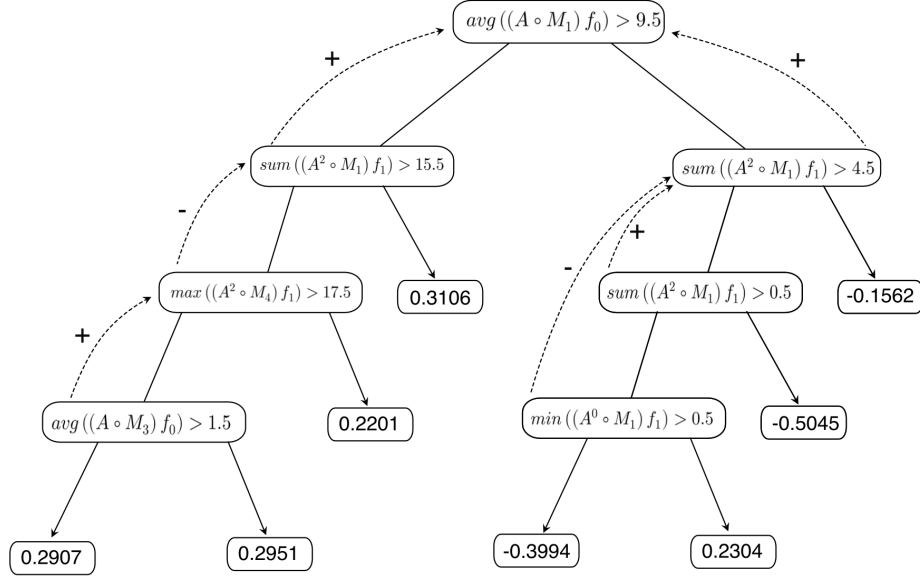


Figure 3: One TREE-G tree in the ensemble of the MUTAG experiment. Each node in the tree contains the chosen split criterion in that node. The dashed arrow in each node points to the split-node where the subset is taken from.

$[0, \dots, 6]$  which encodes the atom it represents, using the following map:  $0 = C, 1 = N, 2 = O, 3 = F, 4 = I, 5 = Cl, 6 = Br$ . Each node in the tree shows the split criterion used in that node. The dashed arrow in each node points to the node in the path to the root where the used subset is taken from. The  $\pm$  near each dashed arrow indicates the value of the parameter  $\rho$ ; i.e., which of the two generated subsets is used. Each graph in the dataset has different vertices, therefore it induces different subsets.

## B Appendix B

The proofs of the lemmas presented in the main paper were skipped due to space limitations. Here we provide the proofs for these lemmas.

### B.1 Proof of Lemma 4.1

**Lemma.** *TREE-G is invariant to permutations in the case of graph labeling and equivariant in the case of vertex labeling.*

We first show that every component in the split criterion of TREE-G is permutation-equivariant, except for the aggregation function applied in the case of graph-level tasks, which is permutation-invariant. Let  $\pi$  be a permutation over the vertices, and  $P_\pi$  the corresponding permutation matrix. For any permutation matrix  $P$ , it holds that  $P^T P = I$ , therefore:

$$\left( P_\pi A P_\pi^T \right)^d (P_\pi \mathbf{f}_k) = \left( P_\pi A P_\pi^T \right) \left( P_\pi A P_\pi^T \right) \dots \left( P_\pi A P_\pi^T \right) (P_\pi \mathbf{f}_k) = P_\pi \left( A^d \mathbf{f}_k \right)$$

and therefore  $A^d \mathbf{f}_k$  is permutation-equivariant.

Similarly, when subsets are used, if one uses a mask  $M$ , the above equivariance similarly holds because:

$$\begin{aligned} \left( \left( P_\pi A P_\pi^T \right)^d \odot \left( P_\pi M P_\pi^T \right) \right) (P_\pi \mathbf{f}_k) &= \left( \left( \left( P_\pi A P_\pi^T \right) \left( P_\pi A P_\pi^T \right) \dots \left( P_\pi A P_\pi^T \right) \right) \odot \left( P_\pi M P_\pi^T \right) \right) (P_\pi \mathbf{f}_k) \\ &= \left( \left( P_\pi A^d P_\pi^T \right) \odot \left( P_\pi M P_\pi^T \right) \right) (P_\pi \mathbf{f}_k) = \left( P_\pi \left( A^d \odot M \right) P_\pi^T \right) (P_\pi \mathbf{f}_k) = P_\pi \left( \left( A^d \odot M \right) \mathbf{f}_k \right) \end{aligned}$$

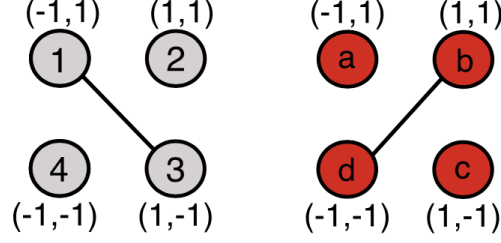


Figure 4:  $G_1$ (red) and  $G_2$ (grey) are two graphs on 4 vertices that are positioned on the plane at  $\{\pm 1\} \times \{\pm 1\}$ . Each graph has two features corresponding to its coordinates. In the proof of Lemma 4.3 we show that these graphs are indistinguishable by TREE-G without subsets, but are separable when subsets are used.

Next, recall that in the case of vertex labeling, the threshold is applied to the vector  $A^d \mathbf{f}_k$  entry-wise. For every  $\theta \in \mathbb{R}$  it holds that

$$\left(A^d \mathbf{f}_k\right)_i \geq \theta \iff P_\pi \left(A^d \mathbf{f}_k\right)_{\pi(i)} \geq \theta$$

therefore thresholding  $A^d \mathbf{f}_k$  is permutation-equivariant. Overall, in the case of vertex labeling, TREE-G’s split criterion is a decomposition of permutation-equivariant functions, and therefore it is permutation-equivariant.

In the case of graph labeling, the elements of the vector  $A^d \mathbf{f}_k$  are aggregated using a permutation-invariant function, and the threshold is applied to the aggregation result. As the vector  $A^d \mathbf{f}_k$  is permutation-equivariant, aggregating over its elements is permutation-invariant:

$$AGG \left( \left( P_\pi A P_\pi^T \right)^d (P_\pi \mathbf{f}_k) \right) = AGG \left( P_\pi \left( A^d \mathbf{f}_k \right) \right) = AGG \left( A^d \mathbf{f}_k \right)$$

Thresholding in this case is permutation-invariant, and therefore for graph labeling tasks TREE-G’s split-criterion is permutation-invariant.

## B.2 Proof of Lemma 4.2

**Lemma.** *The running time of searching the optimal split in TREE-G is linear in the input features.*

Below we compute how many dynamic features are considered at every split-node. Each dynamic feature is defined by the depth of the propagation  $d$ , an input feature  $k$ , and a subset of the vertices. In graph labeling tasks the aggregation function chosen from one of 4 options, is another parameter to consider. Therefore, the computational complexity depends on the number of possible combinations to these parameters. The possible values for  $d$  are bounded by a hyper-parameter we denote here as  $max\_depth$ . The number of subsets that are considered in a split-node  $v$  is at most  $2^{depth(v)} + 1$  where  $depth(v)$  is the depth of the node  $v$  in the tree. This can be further reduced by a hyper-parameter  $a$  that limits a split-node to only consider ancestors that are at distance at most  $a$  from it. This will reduce the number of subsets used to  $2a + 1$  at most. The walks are restricted to the subset in one of at most 4 possible ways. Finally, we have just 4 aggregation functions for graph-level tasks, and no aggregation is used in the case of vertex-level tasks. Overall, in every split, TREE-G computes at most  $4 \times 4 \times (2a + 1) \times max\_depth \times l$  dynamic features. Therefore, the number of dynamic features in each split is linear in the number of input-features  $l$ , as in standard decision trees that only acts on the input features. Notice that during inference it is possible to do a lazy evaluation of dynamic features such that only features that are actually used in the decision process are evaluated.

## B.3 Proof of Lemma 4.3

**Lemma.** *There exist graphs that are separable by TREE-G, but are inseparable if TREE-G is limited to not use subsets.*

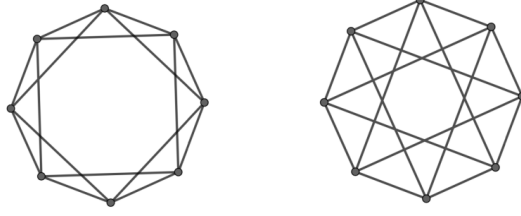


Figure 5: Two 4-regular non-isomorphic graphs. The two graphs differ, for example, in their number of cycles of length 3. The figure is taken from [61]

Consider graphs on 4 vertices that are positioned on the plane at  $\{\pm 1\} \times \{\pm 1\}$  such that each vertex has two features  $\mathbf{f}_1$  and  $\mathbf{f}_2$  corresponding to its  $x$ -axis and  $y$ -axis. We consider two such graphs as presented in Figure 4. Note that for any of the features  $A^0 f$  is identical for  $G_1$  and  $G_2$  since it ignores the edges of these graphs. For  $d \geq 1$  note that  $A^d \mathbf{f}$  is a permutation of the vector  $(1, -1, 0, 0)$  for  $G_1$  and  $G_2$ . Since the aggregation functions are permutation invariant, applying any aggregation function to  $A^d \mathbf{f}$  will generate the same value for  $G_1$  and  $G_2$ . Moreover, since the topology of  $G_1$  and  $G_2$  is isomorphic, any invariant graph-theoretic feature would have the same value of  $G_1$  and  $G_2$ . Therefore, TREE-G without subsets cannot distinguish between  $G_1$  and  $G_2$ . Nevertheless, TREE-G can distinguish between them when using subsets. Specifically, the tree shown in Figure 6 will separate these two graphs to two different leaves. The root of the tree conditions on  $f_1$  which generates a subset of the vertices  $\{(1, 1), (1, -1)\}$ . At the following level, the tree propagates  $f_2$  along walks of length 2 masking on this subset. For  $G_1$ , the only walk that is not masked out is the walk starting and ending in  $(1, 1)$  and therefore for this vertex the value 1 is computed while 0 is computed for all other vertices. However, for  $G_2$ , the only walk of length 2 that is not masked out is the one starting and ending at  $(1, -1)$ . Therefore, in  $G_2$ , the value  $-1$  is computed for the vertex and  $(1, -1)$  and the value 0 is computed for all other vertices. See Figure 7 for a visualization of this analysis.

Therefore,  $(A^2 \odot M_3(\{(1, 1), (1, -1)\})\mathbf{f}_2)$  is a permutation of the vector  $(1, 0, 0, 0)$  for  $G_1$  and a permutation of the vector  $(-1, 0, 0, 0)$  for  $G_2$  and thus TREE-G can distinguish between these graphs.

#### B.4 Proof of Lemma 4.4

**Lemma.** *There exist graphs that cannot be separated by GNNs but can be separated by TREE-G.*

Let  $G_1$ , and  $G_2$  be the two 4-regular non-isomorphic graphs as in Figure 5. Assume that all vertices have the same fixed feature 1. Namely, we wish to distinguish these two graphs only by their topological properties. It is easy to see that a GNN will not be able to distinguish these two graphs, as after the message passing phase, all nodes will result in the same embedding [61]. In contrast, TREE-G is able to separate these two graphs with a single tree consisting of a single split node, by applying the split rule:  $\sum (A^3 \odot M_t(V))f_1 \leq 1$ . This rule counts the number of cycles of length 3 in each graph. Notice that GNNs here refer to the class of MPGNNs [29], whose discriminative power is known to be bounded by the 1-WL test [27]. In particular, popular models such as GIN, GAT and GCN [16, 17, 27], which are also presented in the empirical evaluation sections, all belong to this class of GNNs. GIN [27] with sufficient amount of layers was shown to have exactly the same expressive power as 1-WL.

## C Appendix C

As discussed in the main paper, there are many ways to limit walks to vertices. In TREE-G we use 4 ways that are natural and effective. We now present 4 synthetic tasks, showing that each of these walk types is superior for some task. On each task, we ran 5 experiments. In 4 experiment we used TREE-G where we only allow one type of walks. Then, we compared the lowest loss to TREE-G when we allow 3 types of walks: the 3 types that did not have the lowest loss. The tasks are:

1. Count walks starting in red vertices.

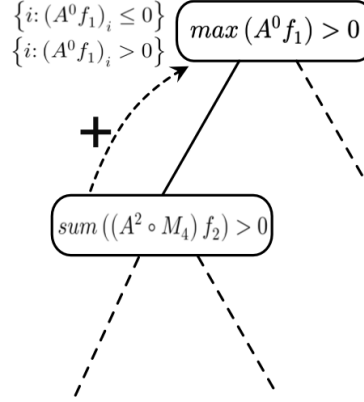


Figure 6: The tree that separates the two graphs  $G_1$  and  $G_2$  in Figure 4.

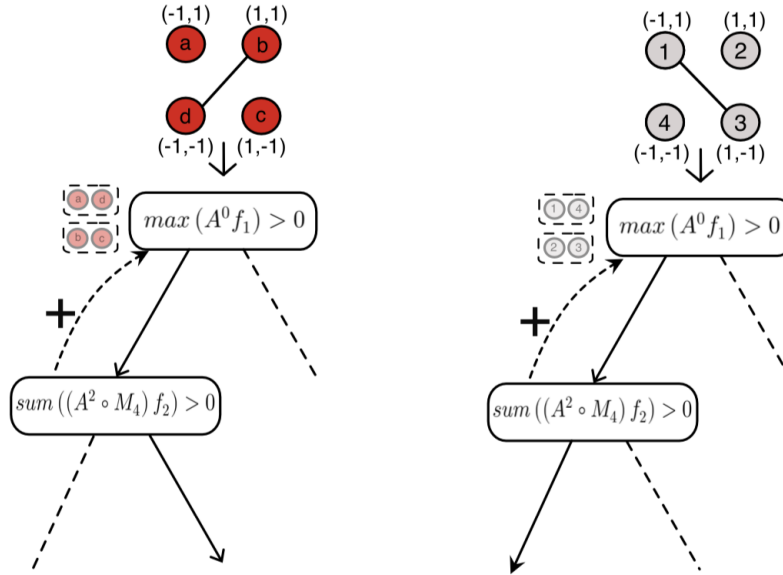


Figure 7: The prediction path of the graphs  $G_1$ (red) and  $G_2$ (grey) in the tree. The path is marked with bold arrows. The available subsets that are generated by the root are marked with a dashed line next to the root edges. The selected subset used in the inner split node is shown left of the node.

2. Count walks starting and ending in the same red vertex.
3. Count walks ending in red vertices.
4. Count walks between red vertices.

In Figures 8, 9, 10, 11 figures, each couple of figures corresponds to one task of the above tasks. In each task, we plot the 4 experiments where only one walk type is used (right subfigures) and the experiment where we allow all 3 types of walk that did not achieve lowest error (left subfigures).

## D Appendix D

In this section, we formalize the explanation mechanism of TREE-G. We show that the selected subsets can be used to explain the predictions made by TREE-G. This explanations mechanism ranks

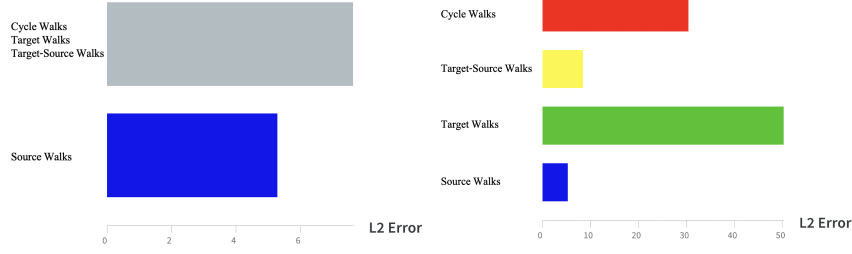


Figure 8: The L2 error of TREE-G on the "count walks starting in red vertices" task, tested with different walk types.

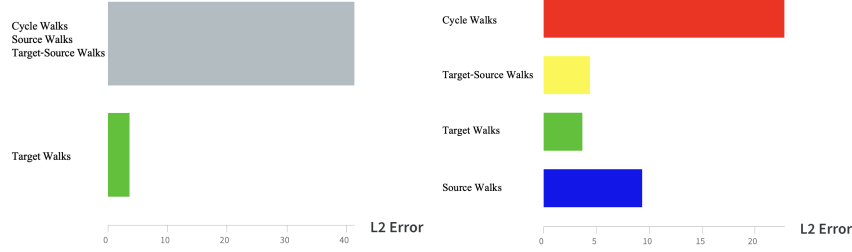


Figure 9: The L2 error of TREE-G on the "Count walks ending in red vertices" task, tested with different walk types.

the vertices and edges of the graph according to their presence in chosen subsets and thus highlights the parts of the graph that contribute the most to the prediction.

Let  $G$  be a graph that we want to classify using a decision tree  $T$ . The key idea in the construction of our importance weight is that if a vertex appears in many selected subsets when calculating the tree output for  $G$ , then it has a large effect on the decision. This is quantified as follows: consider the path in  $T$  that  $G$  traverses when it is being classified. For each vertex  $i$  in  $G$ , count how many selected subsets in the path contain  $i$ , and denote this number by  $n(i)$ . In order to avoid dependence on the size of  $T$  we convert the values  $n_T(1), \dots, n_T(|V|)$  into a new vector  $r_T(1), \dots, r_T(|V|)$  where  $r_T(i)$  specifies the rank of  $n_T(i)$  in  $n_T(1), \dots, n_T(|V|)$  after sorting in decreasing order. For example,  $r_T(i) = 1$  if the vertex  $i$  appears most frequently in chosen subsets compared to any other vertex. We shall use  $2^{-r_T(i)}$  to measure the importance of the rank, so that low ranks have high importance.

Now assume we have an ensemble of decision trees  $\mathcal{T}$  (e.g., generated by GBT). For any  $T \in \mathcal{T}$  in the ensemble let  $y_T$  be the value predicted by  $T$  for the graph  $G$ . We weight the rank importance by  $|y_T|$  so that trees with a larger contribution to the decision have a greater effect on the importance measure. Note that boosted trees tend to have large variability in leaf values between trees in the ensemble [62]. Therefore, the importance-score of vertex  $i$  in the ensemble is the weighted average:

$$importance(i) = \frac{\sum_{T \in \mathcal{T}} |y_T| 2^{-r_T(i)}}{\sum_{j \in |V|} \sum_{T \in \mathcal{T}} |y_T| 2^{-r_T(j)}} \quad . \quad (3)$$

The proposed importance score is non-negative and sums to 1.

**Edge-Level Explanations** Similarly to vertex importance, edge importance can be computed. We use the selected subsets to rank the edges of a given graph by their *importance*. Note that each split criterion uses a subset of the graph's edges, according to  $d$  and the active subset. For example, a split criterion may consider only walks of length 2 to a specific subset of vertices, which induces the *used* edges by the split criterion. Let  $E_1, \dots, E_k$  denote the used edges along the prediction walk  $walk_m(G)$ . We now rank each edge  $e_{(i,j)} \in E$  by  $r_m((i,j)) = |\{j | (i,j) \in E_j\}|$ , i.e., the rank of an edge is the number of split-nodes in the prediction walk that use this edge. The ranks  $r_m(i,j)$  are then combined with the predicted value  $y_m$ , as in Eq.6 in the main paper.

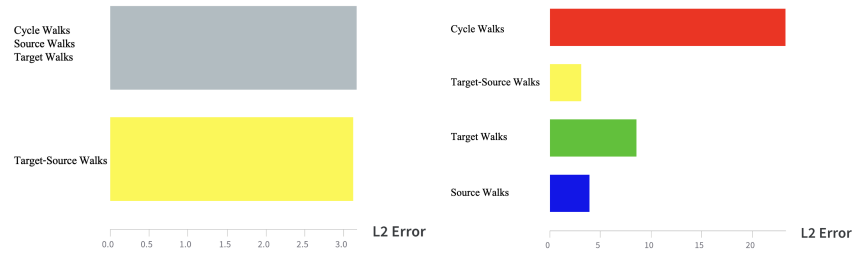


Figure 10: The L2 error of TREE-G on the "Count walks starting and ending in the same red vertex" task, tested with different walk types.



Figure 11: The L2 error of TREE-G on the "Count walks between red vertices" task, tested with different walk types.